Citric acid-modified chitosan hydrogel loaded with shikonin promotes skin wound healing

Authors:

Yuchen Deng*, Chao Wen, Fang Wang

Affiliations:

Shanghai Starriver Bilingual School, Shanghai, China

*Corresponding Author:

Yuchen Deng, Shanghai Starriver Bilingual School, No. 2588, Jindu Road, Minhang District, Shanghai 201100, China.

Tel: +86-15618012209; E-mail: yuchengdeng2008@163.com

Abstract

Background: Despite the advancements of pharmacological treatments and gauze dressings in the field of skin wound healing, these methods present numerous limitations. Therefore, developing a multifunctional material capable of efficiently promoting skin wound healing is particularly crucial.

Methods: Citric acid (CA)-modified chitosan (CS) loaded with Shikonin (SK) (CA-CS-SK) hydrogel was prepared via the freeze-thaw method. The physical properties of the hydrogel were profiled through FTIR, SEM, rotational rheometry, swelling experiment, degradation rate analysis, and drug release experiments. Furthermore, the biocompatibility of the hydrogel was comprehensively evaluated through hemolysis assay, CCK-8 cytotoxicity detection, and live/dead cell staining. Antimicrobial activity against *E. coli* and *S. aureus* of the hydrogel was gauged *in vitro*, and its therapeutic performance was ultimately validated in a mouse full-thickness wound model through H&E staining and ELISA.

Results: The CA-CS-SK hydrogel exhibited appropriate rheological properties, swelling ratio, degradation rate, and drug release rate. It effectively suppressed the proliferation of E.

coli and S. aureus, with superior inhibitory effects compared to CA-CS hydrogel and SK

alone. Additionally, the hydrogel showed no significant toxicity to human dermal fibroblasts

and did not cause erythrocyte rupture. Animal model experiments demonstrated that,

compared to cotton gauze, CA-CS hydrogel, and SK, the CA-CS-SK hydrogel reduced levels

of TNF-α and IL-6 at the wound site, alleviated the inflammatory response, and promoted

wound healing.

Conclusion: The CA-CS-SK hydrogel possesses high antibacterial activity, excellent

biocompatibility, and efficient wound healing promotion capabilities, making it a highly

promising material for skin wound treatment.

Keywords: chitosan, citric acid, shikonin, hydrogel, skin wound

1 Introduction

Skin, the largest organ of the human body, shields us from mechanical damage and

infection, regulates physiological activities, and maintains homeostasis¹. However, when the

skin suffers severe injury, its intrinsic regenerative capacity alone is often insufficient for

healing. Under such circumstances, wounds are readily colonized by viruses, bacteria, and

other pathogens, leading to symptoms such as redness, dehiscence, pus formation, and at

worst death². Existing therapies, including topical pharmacotherapy, gauze dressings, and

autologous skin grafting can alleviate wound symptoms to some extent, but they still exhibit

numerous limitations regarding treatment duration, pain management, and scar formation³.

Therefore, developing a multifunctional material capable of effectively promoting wound

healing is paramount.

In recent years, multifunctional hydrogels have made significant progress in the

biomedical field. Hydrogels are highly water-attracting polymers that form 3-D networks and

can swell upon water absorption but do not dissolve, granting them unique advantages in

wound dressing applications⁴. Moreover, hydrogels satisfy several prerequisites for an ideal

wound dressing, including absorbing exudate, maintaining a moist microenvironment,

facilitating gas exchange, providing antibacterial properties, allowing gentle removal, and

2

minimizing pain during changes^{1, 5}. Polymers for hydrogel preparation are diverse, ranging from natural materials like chitosan (CS), carboxymethyl cellulose, sodium alginate, and synthetic ones like polyacrylic acid, polymethacrylic gelatin, acid, N-isopropylacrylamide¹. Among them, CS is a polysaccharide extracted from natural marine resources (e.g., shrimp shells, crab shells) and possesses multiple excellent physiological functions, including antibacterial activity, biocompatibility, biodegradability, hemostatic capability, anticancer potential, immunomodulatory functions, and wound healing promotion^{6,} ⁷. Therefore, CS and its derivatives are widely used in medical wound dressings. However, the poor water solubility of CS somewhat limits its application in hydrogels⁸. To fully leverage its advantages, CS-based hydrogels still require further modification to enhance their performance and applicability.

Shikonin (SK) is a natural naphthoquinone isolated from the roots of the traditional Chinese medicine Lithospermum erythrorhizon⁹. It exhibits various pharmacological activities such as anti-inflammatory, antibacterial, antiviral, and antitumor activities, while also being able to accelerate wound healing and reduce scar formation¹⁰. Thus, SK shows significant potential in treating dermatitis, psoriasis, skin cancer, and promoting wound healing and scar repair^{10, 11}. Studies show that SK accelerates wound repair by stimulating fibroblast and endothelial cells, promoting angiogenesis and tissue remodeling, thereby accelerating the wound healing process¹²⁻¹⁴. These studies confirm the importance of SK in treating skin-related diseases, but as a lipophilic compound, its poor water solubility results in low bioavailability when applied directly to moist wounds¹⁰. The unique physical properties of hydrogels hold promise for addressing this issue, but their application in wound therapy requires further investigation.

Overall, this study developed a novel hydrogel wound dressing based on citric acid (CA), CS, and SK. The physical properties, biosafety, and antibacterial activity of this dressing were thoroughly explored. Its comprehensive performance as a wound dressing was fully evaluated by establishing a mouse full-thickness skin wound model. This research provided new ideas and methods for the development of novel wound dressings.

2 Materials and methods

2.1 Experimental materials

CA (77-92-9), CS (9012-76-4), and SK (517-89-5) were all provided by Shanghai Aladdin Scientific (China). Cotton gauze was provided by Henan Yadu Medical (China). Additionally, IL-6 ELISA detection kit (E-EL-M0046) and TNF-α ELISA detection kit (E-EL-M3063) were purchased from Wuhan Elabscience Biotechnology (China). Calcein-AM/PI cell viability and cytotoxicity assay kit (C2015M), CCK-8 kit (C0037), and H&E staining kit (C0105S)were all procured from Shanghai Beyotime Biotechnology (China).

2.2 Preparation of CA-CS-SK hydrogel

First, CS was dissolved in a 3% (w/v) acetic acid solution to a final concentration of 2 wt%, after which 0.3 wt% CA was incorporated. Then, 10 mL of the mixture was transferred to a mold, frozen at -20 °C for 12 h. Afterwards, the frozen hydrogel was thawed at room temperature in 0.5 M NaOH solution. The resulting gel was washed with deionized water until reaching neutral pH. Once dried, 0.6 mL of a 3 mg/mL SK solution was evenly applied to the surface of the dried CA-CS hydrogel (10 mg), followed by freeze-drying to prepare the CA-CS-SK hydrogel.

2.3 FTIR analysis of hydrogel chemical structure

The hydrogel's chemical structure was elucidated by FTIR (SHIMADZU, Japan), identifying functional groups. The acquired data were subsequently analyzed using Shimadzu IR Solution FTIR software (SHIMADZU, Japan).

2.4 Scanning electron microscopy (SEM)

Hydrogel morphology was examined with a cold-field emission SEM (JEOL, Japan). After freeze-drying, samples were gold-sputtered and imaged at an accelerating voltage of 15 kV.

2.5 Rotational rheological analysis

Rheological behavior of the hydrogel was evaluated through frequency sweep and strain sweep tests. In the frequency sweep, the storage and loss moduli of the hydrogel were recorded at a constant 1% strain. The scanning frequency was set from 0.1 to 100 rad/s. Strain

sweep was employed to measure the storage and loss moduli at a fixed frequency of 1 Hz, with the strain ranging from 0.01% to 1000%.

2.6 Swelling experiment

To evaluate the swelling ratio, pre-weighed, freeze-dried hydrogel samples (initial weight, W_0) were immersed in PBS at room temperature. After 24 h, the samples were retrieved, their surface moisture gently removed with filter paper, and re-weighed to obtain the swollen weight (W_t). The swelling ratio (W_t) was then calculated as:

$$W\% = (W_t - W_0) / W_0 \times 100\%$$

2.7 Biodegradation

Pre-weighed freeze-dried hydrogels (initial weight = W_0) were incubated at 37 °C in 0.0006 % type I collagenase/PBS. During the 72 h immersion, weights were recorded at various time points (time = t). Samples were rinsed with distilled water, pre-frozen at -80 °C, freeze-dried again, and weighed to record the final weight as W_t . The formula was as follows:

Weight loss (%) =
$$[(W_0-W_t)/W_0] \times 100\%$$

2.8 SK release measurement

The SK release experiment was conducted in 10 mL of PBS at pH 7.4. During the experiment, samples were oscillated at 37 °C. At 1, 2, 4, 6, 12, 24, 48, and 72 hours after initiating SK release, 1 mL of sample solution was removed and replaced with an equal volume of PBS at 37 °C. Released SK was quantified by measuring the absorbance at 275 nm using a high-performance liquid chromatograph with a mobile phase of methanol and water (80:20).

2.9 Cell and bacterial culture

Human dermal fibroblasts (HDFs) (106-05A, MERCK, USA) were cultured in fibroblast growth medium under conditions of 5% CO₂ at 37 °C. *E. coli* (TS306085) and *S. aureus* (TS343490) were provided by Testobio (China) and cultured using LB broth (HB0128, Hopebio, China) and LB agar medium (HB0129-2, Hopebio, China).

2.10 Live/dead cell staining

Following the Calcein-AM/PI kit protocol, cells were allocated into four groups and treated with 50 μ L of either PBS, CA-CS hydrogel (100 μ g/mL), SK (100 μ g/mL), or CA-CS-SK hydrogel (100 μ g/mL). After 24 h of incubation, the staining working solution

was added to each group, gently mixed, and incubated at 37 °C for 15 min. Stained cells were then examined under an inverted microscope.

2.11 CCK-8 cytotoxicity assay

HDFs were plated in a 96-well plate at 5×10³ cells/well and cultured at 37 °C with 5% CO₂ until fully adherent. The medium was then replaced with 200 μL fresh medium containing 100 μg/mL of CA-CS hydrogel, SK solution, or CA-CS-SK hydrogel; untreated cells served as controls. The medium was removed after 24 h. Then, 100 μL of medium with CCK-8 reagent was added. Plates were placed in the incubator for 2 h of culture. Finally, absorbance at 450 nm was measured on a microplate reader (Thermo Scientific, USA), and cell viability was calculated.

2.12 Hemolysis assay

From mice, 3 mL of blood was collected and centrifuged at 2000 rpm for 15 min to separate erythrocytes and serum. The erythrocytes were then washed three times with 1× PBS buffer. After washing, the erythrocyte pellet was diluted with PBS buffer to a 2% (v/v) concentration. Then, a series of concentrations of CA-CS-SK hydrogel (0.1, 0.5, 1, 1.5 mg/mL) were added to the erythrocyte suspension. Control groups included erythrocytes incubated with deionized water (positive control) and erythrocytes incubated with 0.9% sodium chloride (negative control). Samples of each erythrocyte suspension group were incubated at 37 °C for 1 h, followed by centrifugation at 2000 rpm for 15 min. The resulting samples were then photographed.

2.13 In vitro antibacterial experiment

CA-CS hydrogel and CA-CS-SK hydrogel were cut into 1 cm diameter circles. Mixtures were added to a 24-well plate. Each well of a 24-well plate received 1 mL bacterial suspension (1×10^7 colony forming units (CFU)/mL), either alone (control), or mixed with 100 µg/mL CA-CS hydrogel, 100 µg/mL SK, or 100 µg/mL CA-CS-SK hydrogel. The plate was shaken at 220 rpm for 3 h, after which suspensions were diluted to 1×10^3 CFU/mL, spread evenly on agar, and incubated for 24 h. CFUs were then counted.

2.14 Animal model establishment

Full-thickness excisional wounds (1 cm diameter) were created on the backs of anesthetized, depilated BALB/c mice (Hangzhou Ziyuan Laboratory Animal Technology Co.,

Ltd.). Mice were randomized into four groups and wounds were dressed with sterile cotton gauze, CA-CS hydrogel, SK solution, or CA-CS-SK hydrogel. Wound closure was documented photographically on days 0, 3, 7, and 14. All animal protocols were approved by the Experimental Animal Ethics Committee of Zhejiang Luoxi Medical Technology Co., Ltd., Hangzhou, China. (Approval No. LX-4824122703). Every procedure was carried out in strict accordance with relevant guidelines and regulations, including the principles for human research outlined in the Helsinki Declaration and the principles for animal research outlined in the Guide for the Care and Use of Laboratory Animals (8th edition) published by the National Academies Press, USA.

2.15 *In vivo* antibacterial experiment

An infected wound model was created by injecting 20 μ L of *S. aureus* suspension with 1×10^5 bacteria into the wound. Different dressings were then applied for treatment (refer to Section 2.14). After treatment, wound and surrounding tissue were excised and disrupted. Finally, the disrupted samples were plated on LB agar medium for culture. CFU were then calculated.

2.16 H&E staining

At time points of days 3, 7, and 14 after the treatment, the wound and adjacent skin were excised and fixed in 10% formalin solution. After dehydration and paraffin embedding, 5 μ m sections were cut and mounted on slides. Sections were stained using the H&E staining kit and imaged under a microscope.

2.17 ELISA

Skin samples were weighed, mixed with saline in a 1:9 (g/mL) ratio, and homogenized on ice. The homogenate was centrifuged at low temperature, and the supernatant was collected. Finally, the levels of TNF- α and IL-6 were detected with the TNF- α ELISA detection kit and IL-6 ELISA detection kit, respectively.

2.18 Statistical analysis

Data are presented as mean \pm SD (n \geq 3). Statistical comparisons were carried out with GraphPad Prism 8.0. Inter-group differences were assessed by independent sample *t*-tests. p < 0.05 was considered statistically significant.

3 Results

3.1 Preparation and characterization of CA-CS-SK hydrogel

As shown in Figure 1A, SEM imaging revealed that the hydrogel possessed a uniform porous structure with interconnected pores, conducive to drug loading and diffusion. FTIR spectra of CS and the CA-CS complex are shown in Figure 1B. CS exhibited a bending vibration peak at 1590 cm⁻¹ (N-H bend, -NH₂), a stretching vibration broad peak at 3350–3400 cm⁻¹ (O-H/N-H stretch), and a C-O-C glycosidic linkage stretching at 1070 cm⁻¹. CA-CS showed a weakened N-H bending vibration peak at 1590 cm⁻¹, broadened O-H and N-H stretching vibration peaks around 3350–3400 cm⁻¹, and the appearance of symmetric stretching vibration of -COO⁻ near 1400 cm⁻¹, indicating successful incorporation of CA molecules into the CS chain. The drug release results of the hydrogel are shown in Figure 1C. At 72 h, the SK release rate reached 83.4%, indicating good drug release properties. The swelling and degradation experimental results of the hydrogels are shown in Figures 1D and E. Both the blank hydrogel and CA-CS-SK hydrogel swelled rapidly within 5 min, reaching swelling equilibrium around 30 min with a swelling ratio of approximately 300%. The degradation rates of both the blank hydrogel and CA-CS-SK hydrogel were slow, reaching about 45% at 72 h. The SK-loaded hydrogel had increased cross-linking density, resulting in slower swelling and degradation rates compared to the blank hydrogel. Mechanical profiles of the hydrogel, including storage modulus (G') and loss modulus (G"), were obtained by frequency- and strain-sweep rheometry, as shown in Figures 1F and G. Under a constant strain of 1%, the storage modulus (G') dominated the loss modulus (G") over the entire frequency range of 0.1~100 rad/s, confirming gel formation. When the applied strain exceeded 68%, the storage modulus became lower than the loss modulus due to structural disruption, indicating a maximum tolerated strain of 68% for the hydrogel.

3.2 Biosafety assessment

An ideal wound dressing should possess good biocompatibility¹⁵. To evaluate the cytocompatibility of the CA-CS-SK hydrogel, CCK-8 cytotoxicity assessment and live/dead cell staining were performed to analyze its effect on the survival status of HDFs. As shown in **Figure 2A**, in the live/dead cell staining experiment, after staining with Calcein-AM and PI,

HDFs treated with CA-CS hydrogel, SK, or CA-CS-SK hydrogel showed no significant red fluorescence and were not significantly different from the PBS-treated group. This indicated that the survival status of cells in all groups was not significantly inhibited. As shown in **Figure 2B**, in the CCK-8 cell viability assay, the survival rates of HDFs treated with CA-CS hydrogel, SK, and CA-CS-SK hydrogel were 104%, 96%, and 105%, respectively. This demonstrated that the CA-CS-SK hydrogel had good compatibility with HDFs. Furthermore, the study conducted a hemolysis assay, which is an important method for evaluating the hemocompatibility of materials. As shown in **Figure 2C**, erythrocytes in the positive control group (ddH₂O treated) were severely ruptured, showing obvious red coloration in the suspension. In contrast, the 0.9% NaCl (negative control) and different concentrations of CA-CS-SK hydrogel-treated groups showed only slight hemolysis, indicating good hemocompatibility of the CA-CS-SK hydrogel. Therefore, combining the results of cytocompatibility and hemocompatibility, the CA-CS-SK hydrogel exhibited excellent biocompatibility.

3.3 Antibacterial activity assessment

An ideal wound dressing requires not only good biocompatibility but also certain antibacterial capabilities to effectively prevent infection and its spread¹⁵. *E. coli* and *S. aureus* are two common pathogens in the clinical spectrum of wound infections, representing Gram-negative and Gram-positive bacteria respectively¹⁶. To investigate the antibacterial effect of the CA-CS-SK hydrogel, *E. coli* and *S. aureus* were diluted to 1×10³ CFU/mL with PBS. These bacterial suspensions were then spread onto agar plates coated with CA-CS hydrogel, SK, and CA-CS-SK hydrogel, respectively, with untreated plates serving as controls, and incubated at 37 °C for 24 h. As shown in **Figures 3A and B**, for *E. coli*, the survival rates after treatment with CA-CS hydrogel, SK, and CA-CS-SK hydrogel were 74%, 68%, and 26%, respectively. For *S. aureus*, the survival rates were 57%, 43%, and 17%, respectively. These results indicated that both CA-CS hydrogel and SK possessed some ability to inhibit the growth of *E. coli* and *S. aureus*, but the antibacterial effect of the CA-CS-SK hydrogel was the most significant. In summary, the CA-CS-SK hydrogel exhibited good antibacterial abilities.

3.4 Animal model wound healing experiment with CA-CS-SK hydrogel

Building on the previous findings, we next created a full-thickness mouse skin wound model to test the CA-CS-SK hydrogel's capacity to accelerate healing as a wound dressing, benchmarking it against cotton gauze, CA-CS hydrogel alone, and SK alone. As shown in Figure 4A, wounds in all four treatment groups gradually decreased. By day 3 post-wounding, lesions treated with CA-CS hydrogel and SK alone were smaller than those covered with cotton gauze, while wounds treated with CA-CS-SK hydrogel were significantly smaller than those treated with CA-CS hydrogel or SK alone. By day 7, wounds treated with CA-CS hydrogel, SK, and CA-CS-SK hydrogel were all smaller than the cotton gauze group, with the CA-CS-SK hydrogel group showing the smallest wounds. By day 14, wounds in all groups were essentially healed, with the CA-CS-SK hydrogel group showing the best healing outcome. These results indicated that the CA-CS-SK hydrogel effectively promoted skin wound healing, outperforming cotton gauze, CA-CS hydrogel, and SK alone. To further investigate the hydrogel's effect on epidermal and dermal regeneration, wound skin samples from each group were collected on days 3, 7, and 14 post-wounding for H&E staining analysis. As shown in Figure 4B, on day 3, the epidermal layer was severely damaged in all groups, with inflammatory cell infiltration observed in the dermis. By day 7, the cotton gauze group still exhibited significant inflammatory cells within the wound, while the CA-CS hydrogel, SK, and CA-CS-SK hydrogel groups showed markedly reduced inflammatory cells, along with signs of epithelial regeneration, particularly prominent in the CA-CS-SK group. On day 14, inflammatory cells were essentially absent in the CA-CS-SK hydrogel group, and the epidermis was almost completely regenerated. In contrast, the cotton gauze group still showed some inflammatory cell aggregation around the wound, indicating it was still in the tissue remodeling phase. These results demonstrated that both CA-CS hydrogel and SK could promote wound healing, but the CA-CS-SK hydrogel exhibited the most significant effect overall. After injury, damaged skin tissue undergoes a sustained inflammatory response, primarily driven by pro-inflammatory cytokines TNF-α and IL-6, whose excessive levels amplify the toxicity of inflammatory cells and induce the release of more inflammatory mediators, ultimately perpetuating tissue necrosis¹⁷. As shown in **Figure 4C**, ELISA analyses revealed a progressive decline in both cytokines across all groups over 14 days. At every

measured time point (days 3, 7, 14), wounds treated with CA-CS hydrogel, SK alone, or CA-CS-SK hydrogel exhibited significantly lower TNF-α and IL-6 concentrations than gauze controls, with the CA-CS-SK hydrogel producing the sharpest reduction. These results indicated that the CA-CS-SK hydrogel effectively reduced local inflammation and accelerated healing. Additionally, a wound infection model based on *S. aureus* was established to gauge on-site antimicrobial efficacy, as shown in **Figure 4D**. On days 3, 7, and 14 post-treatment, the bacterial survival rates in the CA-CS hydrogel, SK, and CA-CS-SK hydrogel groups were lower than in the cotton gauze group, with the CA-CS-SK group showing the lowest survival rate. Specifically, by day 14 post-treatment, the survival rates in the CA-CS hydrogel, SK, and CA-CS-SK hydrogel groups decreased to 71%, 44%, and 25%, respectively, which demonstrated that the CA-CS-SK hydrogel possessed good antibacterial activity at the skin wound site. In summary, the CA-CS-SK hydrogel demonstrated excellent wound care potential and held promise as a novel high-performance wound dressing material.

4 Discussion

Although current therapeutic approaches have made certain advances in cutaneous wound healing, they still suffer from notable limitations³. Therefore, developing a multifunctional material that can effectively accelerate wound repair is urgently needed. To this end, we designed and developed a CA-CS-SK hydrogel. This hydrogel displayed potent antibacterial activity and pronounced wound-healing efficacy and was expected to become a novel high-performance wound dressing.

SK is a natural compound with diverse biological activities. In addition to anti-inflammatory, antioxidant, antimicrobial, and antitumor properties, SK has been shown to enhance endothelial cell proliferation, migration, and angiogenesis while remodeling the extracellular matrix, thereby accelerating wound healing^{10, 18}. In the present study, we further validated the potential of SK in skin wound repair. Our results confirmed that SK effectively suppressed wound infection and attenuated inflammation, thereby promoting healing, which aligned well with previous reports. For example, SK-loaded liposomes have been reported to inhibit *S. aureus* infection and to alleviate inflammation via modulation of the I-κBα/NF-κB-p65 pathway, thus accelerating burn-wound healing¹⁹. Both that study and ours

demonstrate SK's therapeutic potential in wound management. However, unlike the liposomal formulation, we employed a CA-CS hydrogel as the SK carrier. Skin wound healing is a complex process, and monotherapy often fails to achieve optimal outcomes. Compared with SK-loaded liposomes, CA-CS hydrogel not only retains the inherent advantages of hydrogels, including high absorbency, moisture retention, cooling analgesia, and minimal trauma during dressing changes, but CS itself also promotes platelet adhesion to the vascular wall and platelet aggregation, accelerating clot formation and providing excellent hemostasis^{20, 21}. Moreover, CS stimulates extracellular-matrix synthesis and remodeling and regulates cell proliferation and differentiation, further facilitating wound closure²². Thus, SK delivery via a CS-based hydrogel may synergistically enhance wound healing, a hypothesis that our study substantiated. Animal experiments revealed that neither CA-CS hydrogel nor SK alone was as effective as the CA-CS-SK hydrogel, indicating a clear synergistic benefit between the CS hydrogel and SK. Collectively, our CA-CS-SK hydrogel is a promising therapeutic material for accelerating skin wound repair.

Despite these encouraging advances, several limitations remain. First, our findings were based solely on animal models. While such models can approximate human skin wound healing to a certain extent, physiological and pathological differences between animals and humans persist. Hence, the efficacy and safety of this hydrogel in human wounds require further validation. Second, although we demonstrated the synergistic effect of CA-CS hydrogel and SK, the precise underlying mechanisms remain to be elucidated. These unresolved issues will be the focus of our future investigations.

5 Conclusion

This study innovatively constructed a CA-CS-SK hydrogel. CA formed stable ionic bonds with the amino groups of CS through its carboxylic acid groups, achieving physical cross-linking. FTIR and SEM analyses revealed the chemical structure and microscopic morphology of the hydrogel. Swelling ratio and degradation rate experiments demonstrated that the hydrogel possessed good water absorption capacity and moderate degradability. Leveraging the intrinsic antibacterial capabilities of both CS and SK, the CA-CS-SK hydrogel effectively suppressed *E. coli* and *S. aureus in vitro*, exhibiting excellent antibacterial

properties. Cell experiments and hemocompatibility tests confirmed its safety profile, showing negligible toxicity to HDFs and intact erythrocytes. In the full-thickness mouse wound model, the CA-CS-SK hydrogel accelerated healing significantly beyond cotton gauze, CA-CS hydrogel, and SK alone. The combined merits of excellent antibacterial properties, high biocompatibility, and wound healing promotion capabilities established CA-CS-SK as a promising novel high-performance wound dressing material.

Declarations

Conflict of Interests

The authors have no conflicts of interest to declare.

Data Availability Statement

The data and materials in the current study are available from the corresponding author on reasonable request.

Funding

Not applicable.

Ethics approval and consent to participate

All animal protocols were approved by the Experimental Animal Ethics Committee of Zhejiang Luoxi Medical Technology Co., Ltd., Hangzhou, China. (Approval No. LX-4824122703). Every procedure was carried out in strict accordance with relevant guidelines and regulations, including the principles for human research outlined in the Helsinki Declaration and the principles for animal research outlined in the Guide for the Care and Use of Laboratory Animals (8th edition) published by the National Academies Press, USA.

Author contribution

Yuchen Deng designed the study, developed the methodology, collected and analyzed data, created visualizations, and wrote the initial manuscript. Chao Wen designed the study, provided resources, supervised the project, and revised the manuscript critically. Fang Wang participated in data acquisition, performed statistical analysis, managed resources, prepared figures, and drafted sections of the paper.

References

- (1) Jin, S.; Newton, M. A. A.; Cheng, H.; Zhang, Q.; Gao, W.; Zheng, Y.; Lu, Z.; Dai, Z.; Zhu, J. Progress of Hydrogel Dressings with Wound Monitoring and Treatment Functions. *Gels* **2023**, *9* (9). DOI: 10.3390/gels9090694 From NLM Publisher.
- (2) Yu, P.; Wei, L.; Yang, Z.; Liu, X.; Ma, H.; Zhao, J.; Liu, L.; Wang, L.; Chen, R.; Cheng, Y. Hydrogel Wound Dressings Accelerating Healing Process of Wounds in Movable Parts. *Int J Mol Sci* **2024**, *25* (12). DOI: 10.3390/ijms25126610 From NLM Medline.
- (3) Fu, Z.; Zou, J.; Zhong, J.; Zhan, J.; Zhang, L.; Xie, X.; Zhang, L.; Li, W.; He, R. Curcumin-Loaded Nanocomposite Hydrogel Dressings for Promoting Infected Wound Healing and Tissue Regeneration. *Int J Nanomedicine* **2024**, *19*, 10479-10496. DOI: 10.2147/IJN.S479330 From NLM Medline.
- (4) Nifontova, G.; Safaryan, S.; Khristidis, Y.; Smirnova, O.; Vosough, M.; Shpichka, A.; Timashev, P. Advancing wound healing by hydrogel-based dressings loaded with cell-conditioned medium: a systematic review. *Stem Cell Res Ther* **2024**, *15* (1), 371. DOI: 10.1186/s13287-024-03976-x From NLM Medline.
- (5) Arabpour, Z.; Abedi, F.; Salehi, M.; Baharnoori, S. M.; Soleimani, M.; Djalilian, A. R. Hydrogel-Based Skin Regeneration. *Int J Mol Sci* **2024**, *25* (4). DOI: 10.3390/ijms25041982 From NLM Medline.
- (6) Sheng, W.; Qin, H.; Wang, T.; Zhao, J.; Fang, C.; Zhang, P.; Liu, P.; Udduttula, A.; Zeng, H.; Chen, Y. Advanced phosphocreatine-grafted chitosan hydrogel promote wound healing by macrophage modulation. *Front Bioeng Biotechnol* **2023**, *11*, 1199939. DOI: 10.3389/fbioe.2023.1199939 From NLM PubMed-not-MEDLINE.
- (7) Che, X.; Zhao, T.; Hu, J.; Yang, K.; Ma, N.; Li, A.; Sun, Q.; Ding, C.; Ding, Q. Application of Chitosan-Based Hydrogel in Promoting Wound Healing: A Review. *Polymers (Basel)* **2024**, *16* (3). DOI: 10.3390/polym16030344 From NLM PubMed-not-MEDLINE.
- (8) Qiao, L.; Liang, Y.; Chen, J.; Huang, Y.; Alsareii, S. A.; Alamri, A. M.; Harraz, F. A.; Guo, B. Antibacterial conductive self-healing hydrogel wound dressing with dual dynamic bonds promotes infected wound healing. *Bioact Mater* **2023**, *30*, 129-141. DOI: 10.1016/j.bioactmat.2023.07.015 From NLM PubMed-not-MEDLINE.
- (9) Cen, L. S.; Cao, Y.; Zhou, Y. M.; Guo, J.; Xue, J. W. Shikonin protects mitochondria through the NFAT5/AMPK pathway for the treatment of diabetic wounds. *World J Diabetes* **2024**, *15* (12), 2338-2352. DOI: 10.4239/wjd.v15.i12.2338 From NLM PubMed-not-MEDLINE.
- (10) Song, Y.; Ding, Q.; Hao, Y.; Cui, B.; Ding, C.; Gao, F. Pharmacological Effects of Shikonin and Its Potential in Skin Repair: A Review. *Molecules* **2023**, *28* (24). DOI: 10.3390/molecules28247950 From NLM Medline.
- (11) Rat, A.; Naranjo, H. D.; Krigas, N.; Grigoriadou, K.; Maloupa, E.; Alonso, A. V.; Schneider, C.; Papageorgiou, V. P.; Assimopoulou, A. N.; Tsafantakis, N.; et al. Endophytic Bacteria From the Roots of the Medicinal Plant Alkanna tinctoria Tausch (Boraginaceae): Exploration of Plant Growth Promoting Properties and Potential Role in the Production of Plant Secondary Metabolites. *Front Microbiol* **2021**, *12*, 633488. DOI: 10.3389/fmicb.2021.633488 From NLM PubMed-not-MEDLINE.
- (12) Imai, K.; Kato, H.; Taguchi, Y.; Umeda, M. Biological Effects of Shikonin in Human Gingival Fibroblasts via ERK 1/2 Signaling Pathway. *Molecules* **2019**, *24* (19). DOI: 10.3390/molecules24193542 From NLM Medline.

- (13) Han, H.; Chen, L.; Liang, S.; Lu, J.; Wu, Y.; Wang, X.; Xu, F.; Ge, L.; Xiao, L. PLA-HPG based coating enhanced anti-biofilm and wound healing of Shikonin in MRSA-infected burn wound. *Front Bioeng Biotechnol* **2023**, *11*, 1243525. DOI: 10.3389/fbioe.2023.1243525 From NLM PubMed-not-MEDLINE.
- (14) Xue, C.; Dou, J.; Zhang, S.; Yu, H.; Zhang, S. Shikonin potentiates skin wound healing in Sprague-Dawley rats by stimulating fibroblast and endothelial cell proliferation and angiogenesis. *J Gene Med* **2024**, *26* (1), e3633. DOI: 10.1002/jgm.3633 From NLM Medline.
- (15) Xue, H.; Hu, L.; Xiong, Y.; Zhu, X.; Wei, C.; Cao, F.; Zhou, W.; Sun, Y.; Endo, Y.; Liu, M.; et al. Quaternized chitosan-Matrigel-polyacrylamide hydrogels as wound dressing for wound repair and regeneration. *Carbohydr Polym* **2019**, *226*, 115302. DOI: 10.1016/j.carbpol.2019.115302 From NLM Medline.
- (16) Wang, S. L.; Zhuo, J. J.; Fang, S. M.; Xu, W.; Yu, Q. Y. Silk Sericin and Its Composite Materials with Antibacterial Properties to Enhance Wound Healing: A Review. *Biomolecules* **2024**, *14* (6). DOI: 10.3390/biom14060723 From NLM Medline.
- (17) Prasad, R.; Kapoor, R.; Srivastava, R.; Mishra, O. P.; Singh, T. B. Cerebrospinal fluid TNF-alpha, IL-6, and IL-8 in children with bacterial meningitis. *Pediatr Neurol* **2014**, *50* (1), 60-65. DOI: 10.1016/j.pediatrneurol.2013.08.016 From NLM Medline.
- (18) Tian, M.; Wu, J.; Du, Q.; Han, J.; Yang, M.; Li, X.; Li, M.; Ding, X.; Song, Y. Revealing the Mechanisms of Shikonin Against Diabetic Wounds: A Combined Network Pharmacology and In Vitro Investigation. *J Diabetes Res* **2025**, *2025*, *4656485*. DOI: 10.1155/jdr/4656485 From NLM Medline.
- (19) Shu, G.; Xu, D.; Zhang, W.; Zhao, X.; Li, H.; Xu, F.; Yin, L.; Peng, X.; Fu, H.; Chang, L. J.; et al. Preparation of shikonin liposome and evaluation of its in vitro antibacterial and in vivo infected wound healing activity. *Phytomedicine* **2022**, *99*, 154035. DOI: 10.1016/j.phymed.2022.154035 From NLM Publisher.
- (20) Guo, W.; Ding, X.; Zhang, H.; Liu, Z.; Han, Y.; Wei, Q.; Okoro, O. V.; Shavandi, A.; Nie, L. Recent Advances of Chitosan-Based Hydrogels for Skin-Wound Dressings. *Gels* **2024**, *10* (3). DOI: 10.3390/gels10030175 From NLM PubMed-not-MEDLINE.
- (21) Feng, P.; Luo, Y.; Ke, C.; Qiu, H.; Wang, W.; Zhu, Y.; Hou, R.; Xu, L.; Wu, S. Chitosan-Based Functional Materials for Skin Wound Repair: Mechanisms and Applications. *Front Bioeng Biotechnol* **2021**, *9*, 650598. DOI: 10.3389/fbioe.2021.650598 From NLM PubMed-not-MEDLINE.
- (22) Kou, S. G.; Peters, L.; Mucalo, M. Chitosan: A review of molecular structure, bioactivities and interactions with the human body and micro-organisms. *Carbohydr Polym* **2022**, *282*, 119132. DOI: 10.1016/j.carbpol.2022.119132 From NLM Medline.

Figure Legends

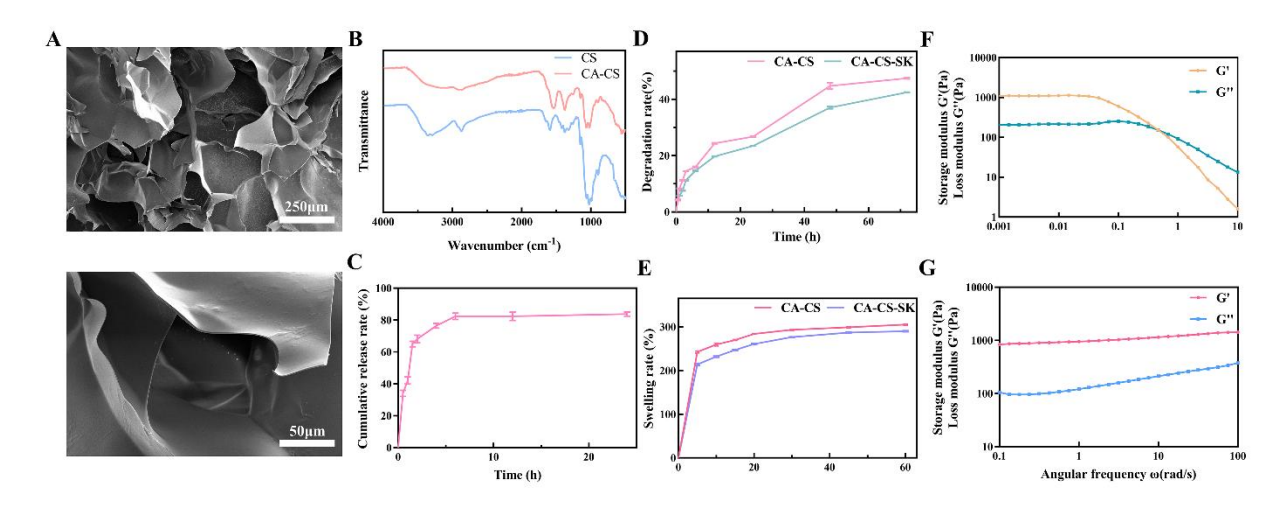


Figure 1 Characterization of CA-CS-SK hydrogel properties.

(A) SEM images of CA-CS-SK hydrogel (Scale bar: 250 μm and 50 μm); (B) FTIR spectra of the hydrogels; (C) Drug release profile of CA-CS-SK hydrogel; (D) Degradation experiment of hydrogels; (E) Swelling experiment of hydrogels; (F) Strain sweep of CA-CS-SK hydrogel; (G) Frequency sweep of CA-CS-SK hydrogel.

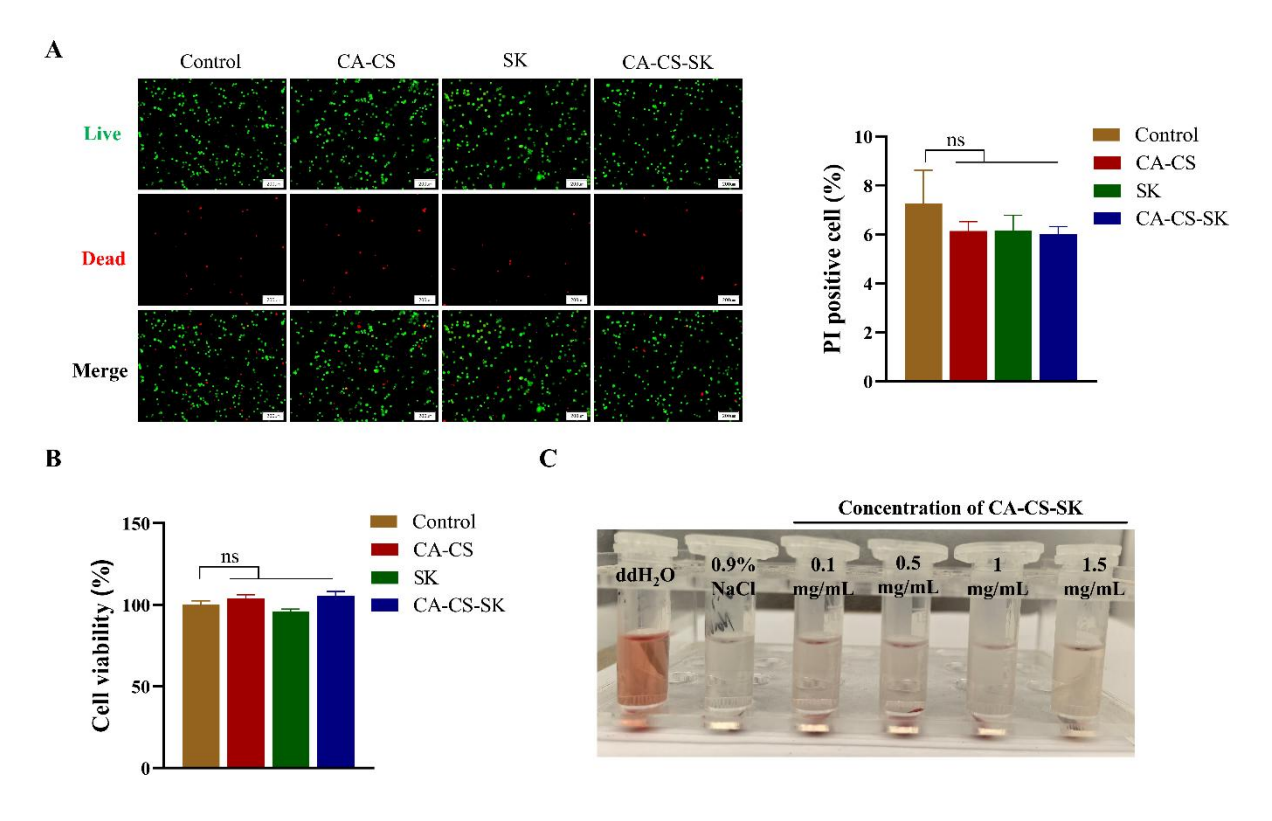


Figure 2 Biosafety assessment.

(A) Live/dead cell staining evaluating the effects of CA-CS, SK, and CA-CS-SK on HDFs; (B) CCK-8 assay evaluating the effects of CA-CS, SK, and CA-CS-SK on HDFs; (C) Hemolysis assay evaluating the hemocompatibility of CA-CS-SK. *p < 0.05.

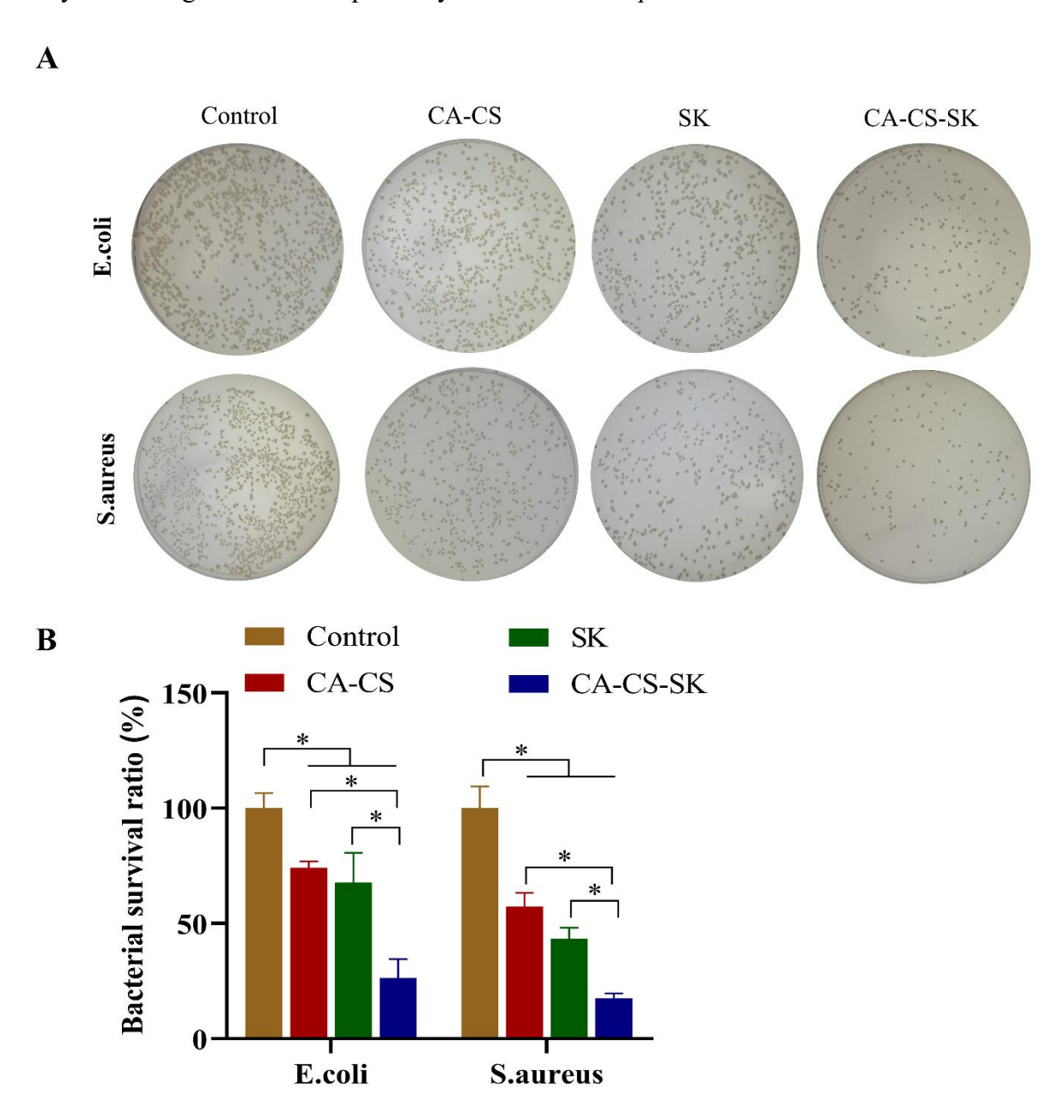


Figure 3 Antibacterial activity assessment.

(A) Antibacterial abilities of hydrogels assessed by CFU counting after co-incubation with E. coli and S. aureus for 24 h; (B) Quantitative analysis of CFU results. *p < 0.05.

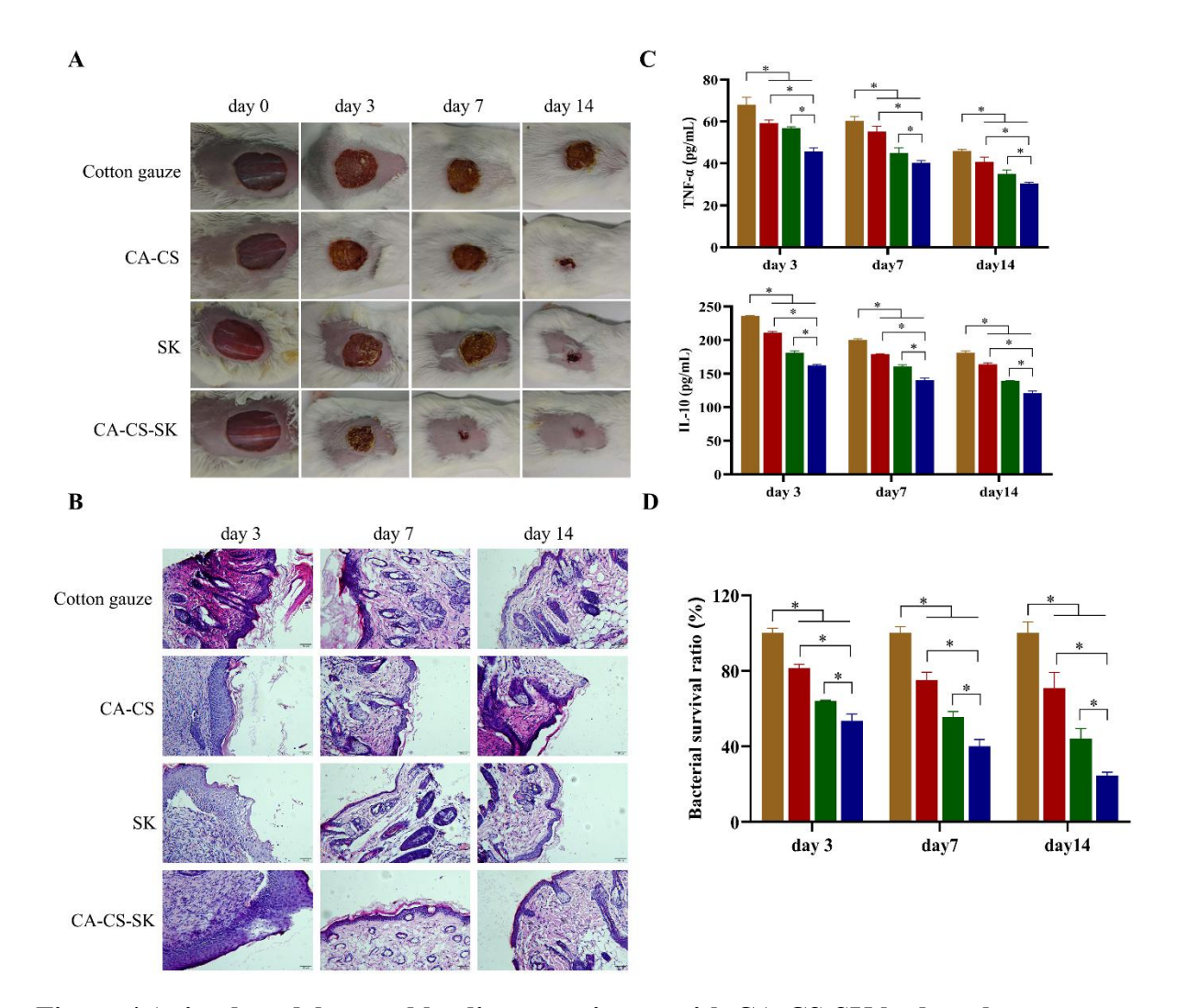


Figure 4 Animal model wound healing experiment with CA-CS-SK hydrogel.

(A) Wound photographs on days 0, 3, 7, and 14 post-wounding; (B) H&E-stained sections of wound tissue on days 3, 7, and 14 post-wounding; (C) Levels of TNF- α and IL-6 in wounds on days 3, 7, and 14 post-wounding; (D) CFU counts of *S. aureus* in wound tissue from each group. *p < 0.05.